

IMPROVEMENT OF THE VISUAL SERVOING TASK WITH A NEW TRAJECTORY PREDICTOR

The Fuzzy Kalman Filter

C. Pérez, N. García, J. M. Sabater, J. M. Azorín and O. Reinoso
Miguel Hernández University, Avda. de la Universidad S/N, Elche, Spain

L. Gracia
Technical University of Valencia, Camino Vera S/N, Valencia, Spain

Keywords: Visual servoing, fuzzy systems, vision / image processing, *Kalman* filter.

Abstract: Visual Servoing is an important issue in robotic vision but one of the main problems is to cope with the delay introduced by acquisition and image processing. This delay is the reason for the limited velocity and acceleration of tracking systems. The use of predictive techniques is one of the solutions to solve this problem. In this paper, we present a Fuzzy predictor. This predictor decreases the tracking error compared with the classic *Kalman* filter (KF) for abrupt changes of direction and can be used for an unknown object's dynamics. The Fuzzy predictor proposed in this work is based on several cases of the *Kalman* filtering, therefore, we have named it: Fuzzy *Kalman* Filter (FKF). The robustness and feasibility of the proposed algorithm is validated by a great number of experiments and is compared with other robust methods.

1 INTRODUCTION

During the last few years, the use of visual servoing and visual tracking has been more and more common due to the increasing power of algorithms and computers.

Visual servoing and visual tracking are techniques that can be used to control a mechanism according to visual information. This visual information is available with a time delay, therefore, the use of predictive algorithms are widely extended (notice that prediction of the object's motion can be used for smooth movements without discontinuities).

The *Kalman* filter (Kalman, 1960) has become a standard method to provide predictions and solve the delay problems (considered the predominant problem of visual servoing) in visual based control systems (Corke, 1998), (Dickmanns and V., 1988) and (Wilson and Bell, 1996).

The time delay is one of the bigger problems in this type of systems. For practically all processing architectures, the vision system requires a minimum delay of two cycles, but for on-the-fly processing, only one cycle of the control loop is needed (Chroust and Vincze, 2003).

Authors of (Chroust and Vincze, 2001) demon-

strate that steady-state *Kalman* filters ($\alpha\beta$ and $\alpha\beta\gamma$ filters) performs better than the KF in the presence of abrupt changes in the trajectory, but not as good as the KF for smooth movements. Some research works about the motion estimation are presented in (S. Soatto and Perona, 1997) and (Z. Duric and Rivlin, 1996). Further, some motion understanding and trajectory planning based on the *Frenet-Serret* formula are described in (J. Angeles and Lopez-Cajun, 1988), (Z. Duric and Rosenfeld, 1998) and (Z. Duric and Davis, 1993). Using the knowledge of the motion and the structure, identification of the target dynamics may be accomplished.

To solve delay problems, taking into account these considerations, we propose a new prediction algorithm, the *fuzzy Kalman filter* (FKF). This filter minimizes the tracking error and works better than the classic KF because it decides what of the used filters ($\alpha\beta^{slow}/\alpha\beta^{fast}$ (Chroust and Vincze, 2003), $\alpha\beta\gamma$, K_v , K_a and K_j) must be employed. The transition between them is smooth avoiding discontinuities.

These five filters should be used in a combination because: The *Kalman* filter is considered one of the reference algorithms for position prediction (but we must consider the right model depending on the object's dynamics: velocity—acceleration—jerk). When

the object is outside the image plane, the best prediction is given by steady-state filters ($\alpha\beta/\alpha\beta\gamma$ depending on the object's dynamics: velocity–acceleration). Obviously, considering more filters and more behaviour cases, FKF can be improved but computational cost of additional considerations can be a problem in real-time execution. These five filters are considered by authors as the best consideration (solution taking into account the prediction quality and the computational cost). This is the reason to combine these five filters to obtain the FKF.

This paper is focused on the new FKF filter and is structured as follows: in section 2 we present the considered dynamics, the considered dynamics is a Jerk model with adaptable parameters obtained by KFs (Nomura and T., 2000), (Li and Jilkov, 2000) and (Mehrotra and Mahapatra, 1997). In section 3, we present the block diagram for the visual servoing task. This block diagram is widely used in several works like (Corke, 1998) or (Chroust and Vincze, 2003). Section 4 presents the basic idea applied in our case (see (Wang, 1997b) and (Wang, 1997a)), but the main work done is focused in one of the blocks described in section 3, the Fuzzy Kalman Filter (FKF) is described in section 5.

In section 6, we can see the results with simulated data. These results show that FKF can be used to improve the high speed visual servoing tasks. This section is organized in two parts: in the first one (Subsection 6.1), the analysis of the FKF behaviour is focussed and in the second one (Subsection 6.2) their results are compared those with achieved by Chroust and Vince (Chroust and Vincze, 2003) and with CPA (Tenne and Singh, 2002) algorithm (algorithm used for aeronautic/aerospace applications). Conclusions and future work are presented in section 7.

2 THE DYNAMICS OF A MOVING OBJECT

The object's movement is not known (a priori) in a general visual servoing scheme. Therefore, it is treated as an stochastic disturbance justifying the use of a KF as a stochastic observer. The KF algorithm presented by Kalman (Kalman, 1960) starts with the system description given by 1 and 2.

$$x_{k+1} = F \cdot x_k + G \cdot \xi_k \quad (1)$$

$$y_k = C \cdot x_k + N \cdot \eta_k \quad (2)$$

where $x_k \in \mathcal{R}^{nx1}$ is the state vector and $y_k \in \mathcal{R}^{mx1}$ is the output vector. The matrix $F \in \mathcal{R}^{n \times n}$ is the so-called system matrix which describes the propagation

of the state from k to $k+1$ and $C \in \mathcal{R}^{m \times n}$ describes the way in which the measurement is generated out of the state x_k . In our case of visual servoing m is 1 (because only the position is measured) and $n = 4$. The matrix $G \in \mathcal{R}^{n \times 1}$ distributes the system noise ξ_k to the states and η_k is the measurement noise. In the KF the noise sequences η_k and ξ_k are assumed to be gaussian, white and uncorrelated. The covariance matrices of ξ_k and η_k are Q and R respectively (these expressions consider 1D movement). A basic explanation for the assumed gaussian white noise sequences is given in (Maybeck, 1982).

In the general case of tracking, the usual model considered is a constant acceleration model (Chroust and Vincze, 2003), but in our case, we consider a constant jerk model described by matrices F and C are:

$$F = \begin{bmatrix} 1 & T & T^2/2 & T^3/6 \\ 0 & 1 & T & T^2/2 \\ 0 & 0 & 1 & T \\ 0 & 0 & 0 & 1 \end{bmatrix}; C = [1 \quad 0 \quad 0 \quad 0]$$

where T is the sampling time. This model is called a *constant jerk model* because it assumes that the jerk ($dx^3(t)/dt^3$) is constant between two sampling instants.

F and C matrices are obtained from expression 3 to 7:

$$\frac{a - a_i}{t - t_i} = \frac{\Delta a}{\Delta t} = J_0 \quad (3)$$

$$x(t) = x_i + v_i(t - t_i) + \frac{1}{2}a_i(t - t_i)^2 + \frac{1}{6}J_0(t - t_i)^3 \quad (4)$$

$$v(t) = v_i + a_i(t - t_i) + \frac{1}{2}J_0(t - t_i)^2 \quad (5)$$

$$a(t) = a_i + J_0(t - t_i) \quad (6)$$

$$J(t) = J_0 \quad (7)$$

where, x is the position, v is the velocity, a is the acceleration and J is the jerk. So the relation between them is:

$$x(t) = f(t); \dot{x}(t) = v(t); \ddot{x}(t) = a(t); \dddot{x}(t) = J(t)$$

3 DESCRIPTION OF THE CONTROL SYSTEM

The main objective of the visual servoing is to bring the target to a position of the image plane and to keep it there for any object's movement. In figure 1 we can see the visual control loop presented by Corke in (Corke, 1998). The block diagram can be used for a moving camera and for a fixed camera controlling the motion of a robot. Corke use a KF to incorporate a feed-forward structure. We incorporate the FKF algorithm in the same structure (see figure 2) but reordering the blocks for an easier comprehension.

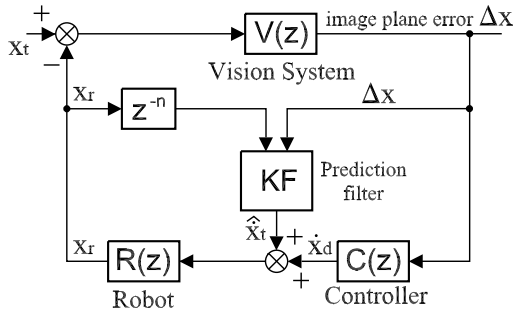


Figure 1: Operation diagram using KF presented by Corke.

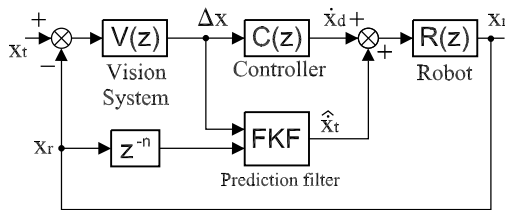


Figure 2: Operation diagram using FKF.

$V(z)$ in figure 2 represents the camera behaviour, which is modeled as a simple delay: $V(z) = k_v \cdot z^{-2}$ (see (Corke, 1998), (Hutchinson and Corke, 1996), (Vincze and Hager, 2000), (Vincze and Weiman, 1997) and (Vincze, 2000)). $C(z)$ is the controller (A simple proportional controller is implemented in experiments presented in this paper). $R(z)$ is the robot (for this work: $R(z) = z/z - 1$) and the *Prediction filter* generates the feedforward signal by prediction the position of the target. The variable for been minimized is Δx (generated by the vision system) that represents the deviation of the target respect to the desired position (error). The controller calculates a velocity signal \dot{x}_d which moves the robot in the right direction to decrease the error. Using this approach, no path planning is needed (the elimination of this path planning is important because it decreases the computational load (Corke, 1998)).

The transfer function of the robot describes the behaviour from the velocity input to the position reached by the camera, which includes a transformation in the image plane. Therefore, the transfer function considered is (Chroust and Vincze, 2003):

$$R(z) = \frac{z}{z-1}$$

The FKF block is explained in the next sections (sections 4 and 5).

4 THEORETICAL BACKGROUND OF THE FUZZY KALMAN FILTER (FKF)

The most common fuzzy inference process used is known as Mamdani's fuzzy inference method, but on the other hand, we can find a so-called *Sugeno*, or *Takagi-Sugeno-Kang*, method of fuzzy inference. It was introduced in 1985 (Sugeno, 1985) and is similar to the Mamdani's method in many respects. The first two parts of the fuzzy inference process, fuzzifying the inputs and applying the fuzzy operator, are exactly the same. The main difference between Mamdani and *Sugeno* is that the *Sugeno* output membership functions are either linear or constant (for more information see (Passino and S., 1988)).

For *Sugeno* regulators, we have a linear dynamic system as the output function so that the i^{th} rule has the form:

If \tilde{z}_1 is \tilde{A}_1^j and \tilde{z}_2 is \tilde{A}_2^k and, ..., and \tilde{z}_p is \tilde{A}_p^l Then $\dot{x}^i(t) = U_i x(t) + V_i u(t)$

where $x(t) = [x_1(t), x_2(t), \dots, x_n(t)]^T$ is the state vector, $u(t) = [u_1(t), u_2(t), \dots, u_m(t)]^T$, U_i and V_i are the state and input matrices and $z(t) = [z_1(t), z_2(t), \dots, z_p(t)]^T$ is the input to the fuzzy system, so:

$$\dot{x}(t) = \frac{\sum_{i=1}^R (U_i x(t) + V_i u(t)) \mu(z(t))}{\sum_{i=1}^R (\mu(z(t)))}$$

or

$$\dot{x}(t) = \left(\sum_{i=1}^R (U_i \xi_i(z(t))) \right) x(t) + \left(\sum_{i=1}^R (V_i \xi_i(z(t))) \right) u(t)$$

where

$$\xi^T = [\xi_1, \dots, \xi_R] = \frac{1}{\sum_{i=1}^R \mu_i} [\mu_1, \dots, \mu_R]$$

Our work is based on this idea and these expressions (see (Passino and S., 1988) for more details). We have mixed the Mamdani's and the *Sugeno*'s idea because we have implemented an algorithm similar to *Sugeno* but not for linear systems. We obtain a normalized weighting of several non linear recursive expressions. The system works like we can see in figure 3 (see section 5).

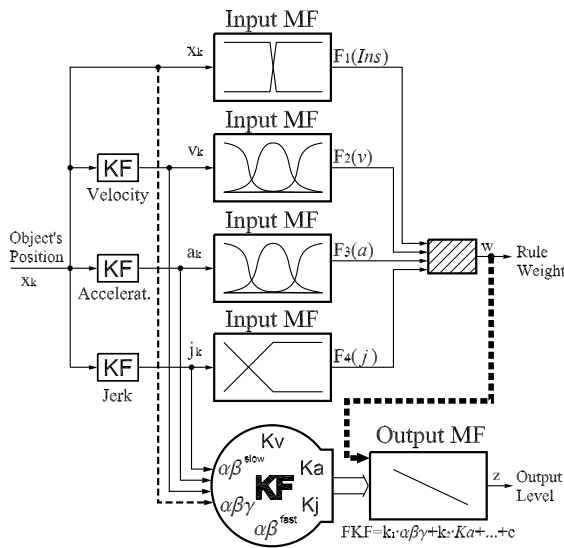


Figure 3: Fuzzy Kalman Filter proposed – FKF.

5 THE FUZZY KALMAN FILTER (FKF)

We have developed a new filter that mixes different types of Kalman filters depending on the conditions of the object's movement. The main advantage of this new algorithm is the non-abrupt change of the filter's output.

Consider the nonlinear dynamic system

$$\dot{x} = f_1(x, u); \quad y = g_1(x, u)$$

as each one of the filters used. The application of the fuzzy regulator in our case produces the next space-state expression:

$$\sum_{i=1}^N f_i(x, u) \cdot \omega(x, u)$$

where

$$\omega(x, u) = \frac{\mu_i(x, u)}{\sum_{i=1}^N \mu_j(x, u)}$$

The final system obtained has the same structure than filters used:

$$\dot{x} = f_2(x, u); \quad y = g_2(x, u)$$

Figure 3 shows the FKF block diagram. In this figure, we can see that the general input is the position sequence of the target (x_k). Using this information, we estimate the velocity, acceleration and jerk of the target in three separate KFs (Nomura and Naito present the advantages of this hybrid technique in (Nomura and T., 2000)). This information is used as 'Input MF' to obtain $F_1(Ins)$, $F_2(v)$, $F_3(a)$ and $F_4(j)$. These MF inputs are the fuzzy membership functions defined in

figure 4. The biggest KF block (rounded) shown in his figure is a combination of all used algorithms in the fuzzy filter ($\alpha\beta^{slow}$ and $\alpha\beta^{fast}$ (Chroust and Vincze, 2003), $\alpha\beta\gamma$, K_v , K_a and K_j). This block obtains the output of all specified filters. The 'Output MF' calculates the final output using the R_i rules.

Now, we present the rules (R_i) considered for the fuzzy filter:

R_1 : IF object IS inside AND velocity IS low AND acceleration IS low AND jerk IS low THEN $FKF=K_v$

R_2 : IF object IS inside AND velocity IS medium AND acceleration IS low AND jerk IS low THEN $FKF=K_v$

R_3 : IF object IS outside AND velocity IS low AND acceleration IS low AND jerk IS low THEN $FKF=\alpha\beta^{slow}$

R_4 : IF object IS outside AND velocity IS medium AND acceleration IS low AND jerk IS low THEN $FKF=\alpha\beta^{fast}$

R_5 : IF object IS inside AND velocity IS high AND acceleration IS low AND jerk IS low THEN $FKF=K_v$

R_6 : IF object IS inside AND acceleration IS medium AND jerk IS low THEN $FKF=0.2 \cdot \alpha\beta\gamma + 0.8 \cdot K_a$

R_7 : IF object IS outside AND acceleration IS medium AND jerk IS low THEN $FKF=0.8 \cdot \alpha\beta\gamma + 0.2 \cdot K_a$

R_8 : IF object IS inside AND acceleration IS high AND jerk IS low THEN $FKF=K_a$

R_9 : IF object IS outside AND acceleration IS high AND jerk IS low THEN $FKF=\alpha\beta\gamma$

R_{10} : IF jerk IS high THEN $FKF=K_j$

These rules have been obtained empirically, based on the authors experience using the Kalman filter in different applications.

Notice that rule R_{10} (when jerk is high) shows that the best filter considered is K_j and it does not depend on the object's position (inside or outside) velocity/acceleration value (low, medium or high).

We have used a product inference engine, singleton fuzzifier and centre average defuzzifier. Figure 4 presents the fuzzy sets definition where (u_{max}, v_{max}) is the image size, $\mu_{vel} = \mu_{acc} = 2m/s$, $\sigma_{vel} = \sigma_{acc} = 0.5$, $c_{vel} = c_{acc} = 1$, $d_{vel} = d_{acc} = 3$, $i_{vel} = i_{acc} = 1$ and $j_{vel} = j_{acc} = 1$ (these values have been empirically obtained).

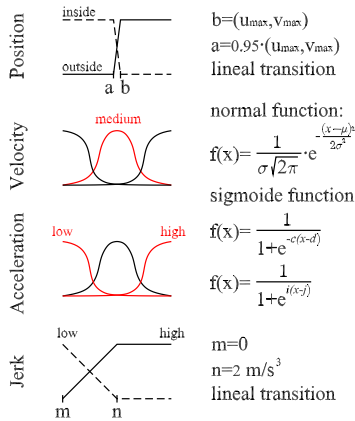


Figure 4: Parameter definition of the fuzzy system.

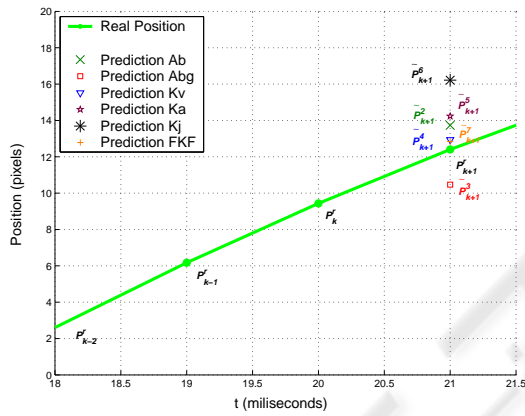


Figure 5: Real position vs. prediction.

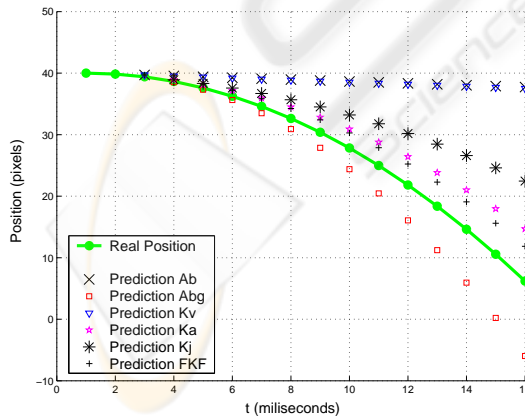


Figure 6: Prediction of a smooth trajectory.

6 RESULTS

This section is composed by two different parts: first (section 6.1), we analyze the prediction algorithm presented originally in this paper (FKF block diagram shown in figure 3) and second (section 6.2), some simulations of the visual servoing scheme (see figure 2) are done including the FKF algorithm.

6.1 Fuzzy Kalman Filter (FKF) Results

In figure 5, we show the effectiveness of our algorithm's prediction compared with the classical KF methods. In this figure, we can see positions P_k^r (actual object position), P_{k-1}^r (object position in $k-1$) and P_{k-2}^r (object position in $k-2$). Next real position of the object will be P_{k+1}^r , and points from \tilde{P}_{k+1}^1 to \tilde{P}_{k+1}^6 , represent the prediction obtained by each single filter. The best prediction is given by the FKF filter. This experiment is done for a parabolic trajectory of an object affected by the gravity acceleration. (See figures 5 and 6).

We have done a lot of experiments for different movements of the object and we have concluded that our FKF algorithm works better than the others filters compared (filters compared are: $\alpha\beta$, $\alpha\beta\gamma$, Kv , Ka , Kj and CPA -see section 6.2- with our FKF). Figure 6 shows the real trajectory and the trajectory predicted for each filter. For this experiment, we have used the first four real positions of the object as input for all filters and they predict the trajectory using only this information. As we can see in this figure, the best prediction is again the FKF.

6.2 Visual Servoing Control Scheme Results

To prove the control scheme presented in figure 2, we have used the object motion shown in figure 7 (up). This target motion represents a ramp-like motion between $1 < t < 4$ seconds and a sinusoidal motion for $t > 6$ seconds. This motion model is corrupted with a noise of $\sigma=1$ pixel. This motion is used by Stefan Chroust and Markus Vincze in (Chroust and Vincze, 2003) to analyze the *switching Kalman filter* (SKF).

For this experiment, we compare the proposed filter (FKF) with a well known filter, the *Circular Prediction Algorithm* (CPA) (Tenne and Singh, 2002). In figure 7 (down), we can see the results of FKF and CPA algorithms. For changes of motion behaviour, the FKF produce less error than CPA. For the change in $t=1$, the FKF error is $[+0.008, -0]$ and $[+0.015, -0.09]$ for the CPA. For the change in $t=4$, FKF error =

Table 1: Numerical comparative for dispersion value of all filters implemented (bounce of a ball experiment).

Init. pos.	$\alpha\beta$	$\alpha\beta\gamma$	Kv	Ka	Kj	FKF
40	0.619	0.559	0.410	0.721	0.877	0.353
40(bis)	0.547	0.633	0.426	0.774	0.822	0.340
50	0.588	0.663	0.439	0.809	0.914	0.381
70	0.619	0.650	0.428	0.700	0.821	0.365
90	0.630	0.661	0.458	0.818	0.857	0.343
150	0.646	0.682	0.477	0.848	0.879	0.347

$[+0, -0.0072]$ and CPA error = $[+0.09, -0.015]$. For the change in $t=6$, FKF error = $[+0.022, -0]$ and CPA error = $[+0.122, -0.76]$. For the region $6 < t < 9$ (sinusoidal movement between 2.5m and 0.5m) both algorithms works quite similarly: FKF error = $[\pm 0.005]$ and CPA error = $[\pm 0.0076]$. CPA filter works well because it is designed for movements similar to a sine shape, but we can compare this results with the SKF filter proposed in (Chroust and Vincze, 2003) and SKF works better (due to the AKF (Adaptive Kalman Filter) effect). Therefore, the FKF filter proposed works better than CPA for all cases analyzed but comparing FKF with SKF, FKF is better for $t=1$, $t=4$ and $t=6$ but not for $6 < t < 9$ (sinusoidal movement).

Figure 9 shows the zoom region $0 < t < 2$ and $-0.02 < \Delta x_p < 0.02$ of the same experiment. In this figure, we can see the fast response of the FKF proposed.

6.3 Experimental Results

Experimental results are obtained for this work using the following setup: Pulnix GE series high speed camera (200 frames per second), Intel PRO/1000 PT Server Adapter card, 3.06GHz Intel processor PC computer, *Windows XP Professional* O.S. and *OpenCV* blob detection library.

For this configuration, the bounce of a ball on the ground is processed to obtain data shown in figure 10. Results of this experiment are presented in table 1. In this table, we can see the dispersion of several filters. The FKF dispersion is less than $\alpha\beta$, $\alpha\beta\gamma$, Kv , Ka and Kj although FKF is a combination of them. This table contains data from this particular experiment (the bounce of a ball on the ground). For this experiment, the position of the ball is introduced to the filters to prove the behaviour of them. The filter proposed (FKF) is the best analyzed.

In figure 11 we can see some frames of the experiment 'bounce of a ball on the ground'. For each frame the center of gravity of the tennis ball is obtained.

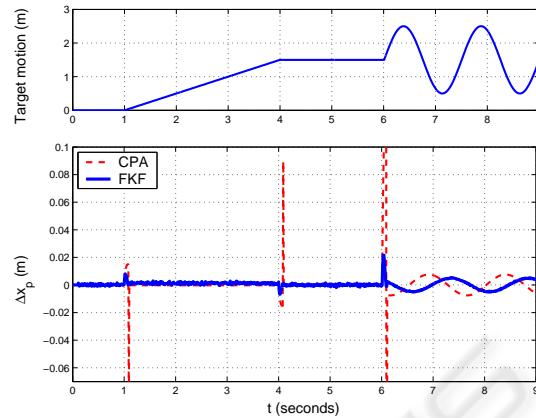


Figure 7: Simulation result for tracking an object.

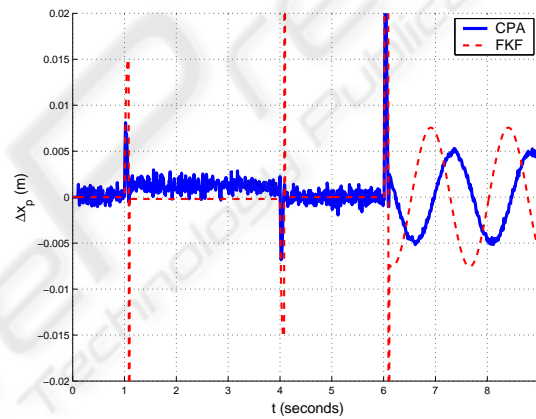


Figure 8: Zoom of the simulation.

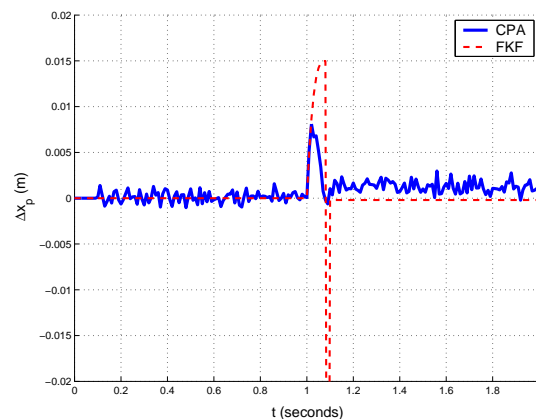


Figure 9: Zoom between 0 and 2 seconds.

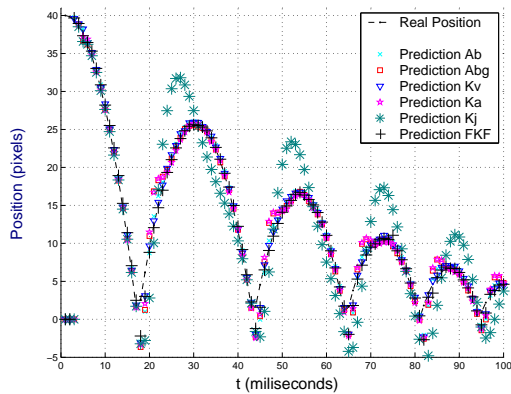


Figure 10: Bounce of the ball on the ground. Data.



Figure 11: Bounce of the ball on the ground. Frames.

7 CONCLUSIONS AND FUTURE WORK

In section 6.1 (figures 5 and 6), we can see the quality of the new filter presented (FKF) which shows good behaviour for smooth and discontinuous motions. The object's position is estimated even when it is inside the image plane and when it is outside the image plane. Therefore, combine classic filters (KF) when inside and steady-state filters ($\alpha\beta/\alpha\beta\gamma$) when outside.

We have compared our filter with $\alpha\beta$, $\alpha\beta\gamma$, Kv , Ka and Kj in experiments of pure prediction. We have compared too, our filter with *Circular Prediction Algorithm* (CPA) in this paper reproducing the same experiment as (Chroust and Vincze, 2003) for a direct comparison with the work done by Chroust and Vincze. The filter proposed works very well but not better than SKF for all conditions, therefore, the addition of a AKF action can improve the filter behaviour (future work).

The FKF is evaluated with a ramp-like and sinusoidal motions. Δx_p is reduced in all tests done and the overshoot is decreased significantly. Results presented in this paper are obtained for $C(z) = K_P$. Other controllers like PD, PID, ... will be implemented in future work.

ACKNOWLEDGEMENTS

This work is supported by the *Plan Nacional de I+D+I 2004-2007*, DPI2005-08203-C02-02 of the Spanish Government (*Técnicas Avanzadas de Teleoperación y Realimentación Sensorial Aplicadas a la Cirugía Asistida por Robots*).

REFERENCES

- Chroust, S. and Vincze, M. (2003). Improvement of the prediction quality for visual servoing with a switching kalman filter. *I. J. Robotic Res.*, 22(10-11):905–922.
- Chroust, S., Z. E. and Vincze, M. (2001). Pros and cons of control methods of visual servoing. In *In Proceedings of the 10th International Workshop on Robotics in the Alpe-Adria-Danube Region*.
- Corke, P. I. (1998). *Visual Control of Robots: High Performance Visual Visual Servoing*. Research Studies Press, Wiley, New York, 1996 edition.
- Dickmanns, E. D. and V., G. (1988). Dynamic monocular machine vision. In *Applications of dynamic monocular machine vision*. Machine Vision and Applications.

- Hutchinson, S., H. G. D. and Corke, P. (1996). Visual servoing: a tutorial. In *Transactions on Robotics and Automation*. IEEE Computer Society.
- J. Angeles, A. R. and Lopez-Cajun, C. S. (1988). Trajectory planning in robotics continuous-path applications. In *Journal of Robotics and Automation*. IEEE Computer Society.
- Kalman, R. E. (1960). A new approach to linear filtering and prediction problems. In *IEEE Transactions on Pattern Analysis and Machine Intelligence*. IEEE Computer Society.
- Li, X. and Jilkov, V. (2000). A survey of maneuvering target tracking: Dynamic models. In *Signal and Data Processing of Small Targets*. The International Society for Optical Engineering.
- Maybeck, P. S. (1982). *Stochastic Models, Estimation and Control*. Academic Press, New York.
- Mehrotra, K. and Mahapatra, P. R. (1997). A jerk model for tracking highly maneuvering targets. In *Transactions on Aerospace and Electronic Systems*. IEEE Computer Society.
- Nomura, H. and T., N. (2000). Integrated visual servoing system to grasp industrial parts moving on conveyor by controlling 6dof arm. In *International Conference on Systems, Man, and Cybernetics*. IEEE Computer Society.
- Passino, K. M. and S., Y. (1988). *Fuzzy Control*. Addison-Wesley, Ohio, USA.
- S. Soatto, R. F. and Perona, P. (1997). Motion estimation via dynamic vision. In *IEEE Transactions on Automatic Control*. IEEE Computer Society.
- Sugeno, M. (1985). *Industrial applications of fuzzy control*. Elsevier Science Publications Company.
- Tenne, D. and Singh, T. (2002). Circular prediction algorithms-hybrid filters. In *American Control Conference*. IEEE Computer Society.
- Vincze, M. (2000). Real-time vision, tracking and control-dynamics of visual servoing. In *International Conference on Robotics and Automation*. IEEE Computer Society.
- Vincze, M. and Hager, G. D. (2000). *Robust Vision for Vision-Based Control of Motion*. SPIE Press / IEEE Press, Bellingham, Washington.
- Vincze, M. and Weiman, C. (1997). On optimizing window-size for visual servoing. In *International Conference on Robotics and Automation*. IEEE Computer Society.
- Wang, L.-X. (1997a). *Course In Fuzzy Systems and Control*, A. Prentice Hall.
- Wang, L.-X. (1997b). *Course in Fuzzy Systems and Control Theory*. Pearson US Imports & PHIPES. Pearson Higher Education.
- Wilson, W. J., W. H. C. C. and Bell, G. S. R. (1996). Relative end-effector control using cartesian position based visual servoing. In *IEEE Transactions on Robotics and Automation*. IEEE Computer Society.
- Z. Duric, E. R. and Davis, L. (1993). Egomotion analysis based on the frenet-serret motion model. In *Proceedings of the 4th International Conference on Computer Vision*. IEEE Computer Society.
- Z. Duric, E. R. and Rosenfeld, A. (1998). Understanding the motions of tools and vehicles. In *Proceedings of the Sixth International Conference on Computer Vision*. IEEE Computer Society.
- Z. Duric, J. A. F. and Rivlin, E. (1996). Function from motion. In *Transactions on Pattern Analysis and Machine Intelligence*. IEEE Computer Society.